Understanding the Structure and Properties of Phase Change Materials for Data Storage Applications

*M. Anbarasu and Matthias Wuttig**

Abstract | Phase change materials possess a unique property combination which is the basis for their application potential. The amorphous and crystalline phases are characterised by very different optical and electrical properties. This is indicative of a significant structural rearrangement upon the phase transition. Nevertheless, it is possible to rapidly and reversibly switch between the amorphous and crystalline states. This property portfolio has already been successfully employed in rewritable optical data storage. Phase change materials are also considered to be one of the most promising candidates for future electronic memories. Hence, considerable efforts have been undertaken in the past decades to identify suitable materials, and to optimize them with respect to specific applications. This article reviews the structure and the underlying bonding mechanism of phase change materials. This understanding of the bonding mechanism and the resulting atomic arrangement will subsequently be utilized to explain several of the characteristic features of phase change materials. Finally, the technological development both of rewritable optical storage media and future non-volatile electronic memories are reviewed.

1. Introduction

In everyday life, the data density of storage media has increased enormously in the past decades. This rapid increase is driven both by novel multimedia applications and the tremendous increase of knowledge and information in the modern world. A wide range of commercially available data storage technologies meet this demand, one of the most successful among them being optical data storage. In the past decades, initially only two different classes of rewritable optical storage media were commercialized, namely magneto-optical and phase change memories. However, in the last decade, phase change materials (PCM) have been utilized in leading rewritable optical data storage technology.[1,2] This is based on the rapid reversible switching between an amorphous and a crystalline state. Both phases are characterized by very different material properties, thus providing the contrast required to distinguish between different logical states.

It is the state-of-the-art technique for rewritable optical storage. In the last decades, optical storage products with continuously increasing storage density ranging from 650 MB (CD-RW) to 33 GB (Blu-ray Disc) have been developed.[1] Their pronounced property contrast, however, can also be used in other memory devices. Since the amorphous and crystalline states have very different electrical resistivities as well, they show potential for applications as electronic memories. Particularly attractive is their excellent scaling.[3] Hence, electronic phase change memories are

Institute for Physics (IA) and JARA-Fundamentals of Future Information Technology, RWTH Aachen University, 52056-Aachen, Germany
**wuttig@physik.rwth-aachen.de*

Flash memory: A type of non-volatile electronic memory that can be electrically erased and reprogrammed. Flash (both NAND and NOR type) memory stores information in an array of memory cells made from floating-gate transistors.

Dynamic random-access memory (DRAM): DRAM is a type of random-access memory that stores each bit of data in a separate capacitor within an integrated circuit. The two logic states of digital '0' or '1' represent the charge state of the capacitor, i.e. if it is charged or discharged. Since capacitors leak charge, the information eventually fades unless the capacitor is refreshed periodically. Because of this refresh requirement, it is called dynamic memory.

considered to be one of the most promising potential successors of *Flash memory*. The rapid switching speeds might even enable a very fast, non-volatile electronic memory, which could provide *DRAM-like speeds*.[4,5] To fully exploit the potential of these storage media, an in-depth understanding of the physical properties of phase change materials is indispensable. In the following pages, this insight will be derived from an understanding of the atomic arrangement and the underlying bonding mechanism in the different states. It is therefore, the aim of this article to review the evolution and the current state of understanding of phase change materials and their technological advancements.

2. Principle of phase change recording

The storage concept used in phase change materials is based on a change in optical and electronic properties that occurs upon the atomic rearrangement which accompanies the transition between the crystalline and the amorphous phases. Figure 1 illustrates the principle of phase change recording.[6] A confined region of amorphous or crystalline material is exposed to a precisely controlled laser pulse or electrical pulse which enables a fast transition between an amorphous and a crystalline state on a nanosecond timescale. This transformation is accompanied by a pronounced change of optical and electronic properties which allows the storage of information. By employing suitable optical or electronic pulses, this transformation between the amorphous and the crystalline phase can be triggered. In both cases, the response of the material is controlled by the temperature rise and length of the stimulus.[1] Starting from a crystalline bit, the temperature first needs to be elevated above the liquidus temperature T_l using an appropriately chosen short, high intensity (high current) pulse during which a spatially confined region is heated up and molten. This leads to a huge temperature gradient between the molten bit and the surrounding material. Subsequently, high cooling rates (of about 10^{10} K/s) bypass the crystallization and a melt-quenched amorphous bit is formed. In this low temperature regime, the atomic mobility is so small that crystallization, though energetically favourable, is kinetically hindered. To switch from the amorphous phase back to the crystalline state, the temperature of the bit needs to be elevated for a sufficiently long time to enable crystallization. To do so, the region to be crystallized has to be heated well above the glass transition temperature.

Figure 1: The principle of operation of phase-change devices is based on the reversible switching between the crystalline and amorphous state. Amorphization (also called RESET-operation) of a bit proceeds via melt-quenching, employing short current pulses as heat sources. In optical recording, short laser pulses are utilized instead. The resulting huge temperature difference between the confined melt and the surrounding material leads to extremely high cooling rates. Thus, the disorder of the liquid is frozen in. Crystallization (SET-operation) requires annealing of an amorphous bit at a temperature below the melting temperature for the atoms to adopt an energetically favorable crystalline order. Reproduced from ref.[1]

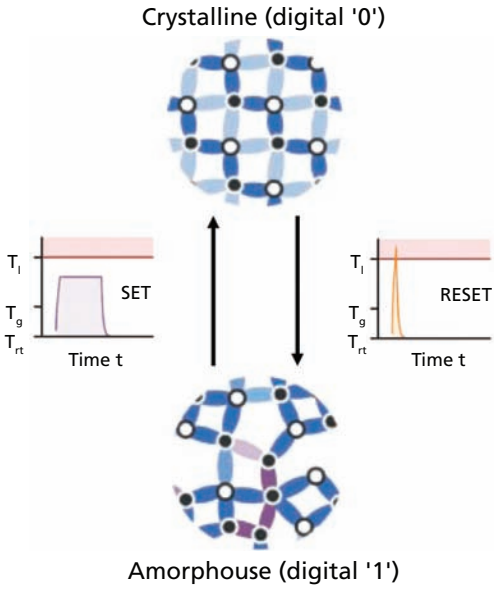

Property contrasts in the local active volume of amorphous or crystalline bits are realized in terms of electrical conductivity (more than three orders of magnitude) or optical reflectivity (up to 30% change, depending on layer thickness and wavelength).[1] To read out whether a bit is amorphous or crystalline, low intensity (low current) pulses are employed to distinguish between low and high reflectivity (conductivity), which encodes the digital information. Noteworthy are the timescales of phase changes. Typically, crystallization is the slowest process involved. Nevertheless, phase change materials re-crystallize very fast, as these alloys represent poor glass formers.[7] Thus, they can be rapidly switched between the two states in a few nanoseconds. After the identification of materials which showed sufficiently rapid crystallization, rewritable optical storage media advanced rapidly.[16] Subsequent material optimization helped to realize several generations of optical storage media. This development will be discussed below.

3. An evolution of PCM and their families

The starting point for the development of storage concepts employing chalcogenides was the discovery of reversible electrical switching

phenomena[8] in chalcogenide glasses. Since then, there has been a tremendous effort spent on understanding this phenomenon and nurturing this peculiar property of memory-switching effects into electronic memory applications.[9,10] The first materials used were good glass formers such as Te-based eutectic alloys, doped with Sb, S and P etc.[8,11] Although these materials showed reversible electrical switching that could be used for electronic storage, the time for crystallization was in the order of microseconds, partly because these first alloys did not crystallize in a single phase. This imposed several limitations on device performance like speed, and repeatability (cyclability). Hence, no commercially viable developments were achieved until the mid-1980s.

A major breakthrough was reached when the first materials to show rapid re-crystallization and good optical contrast (GeTe[12] and $Ge_{11}Te_{60}Sn_4Au_{25}$) were identified.[13,14] Shortly afterwards, the excellent properties of materials along the pseudo-binary line between GeTe and Sb_2Te_3 were discovered.[15,16] The identification of single phase material with rapid crystallization kinetics[17] enabled the realization of rewritable optical data storage. Their property portfolio includes the ability to be switched rapidly between the amorphous and crystalline phases. These two states possess significantly different optical or electrical properties. This property combination ensures the rapid transformation between two distinguishable states. In the past two decades, a number of materials have been identified empirically which have the required properties.

These materials are frequently grouped in different families. Most of the families of phase change materials identified recently can be found in the ternary phase diagram as shown in figure 2, where three different families are discernible. The most prominent materials such as $Ge_2Sb_2Te_5$ or $Ge_1Sb_2Te_4$ are located on the pseudo-binary line between GeTe and Sb_2Te_3 (family I).[16] Besides Sb_2Te_3, Sb_2Te also offers suitable properties when combined with In and/or Ag. A well-known example is AgInSbTe (family II), a material which frequently has a composition close to $Ag_5In_5Sb_{60}Te_{30}$ (AIST).[18] Another material family that has attracted considerable interest in the last few years is based on doped (or better 'alloyed') Sb such as $Ge_{15}Sb_{85}$ (family III).[19,20] This family stands out as it does not contain any chalcogen component. We will demonstrate later on why this finding helps in developing a simple scheme to identify potential phase change materials. Finally, very recently, another new phase change material has been identified with the composition of $In_3Sb_1Te_2$. This is the only material which cannot be represented in the phase diagram of figure 2. Possibly this material is a member of a fourth family of phase change materials.[21]

The next section addresses the structures of crystalline phase change materials and subsequently relates them to the bonding mechanism utilized. Understanding the structure and the related bonding will help to explain the resulting properties and can be used to optimize phase change materials for different applications.

Figure 2: Ternary phase diagram depicting different phase change alloys. Reproduced from ref.[1]

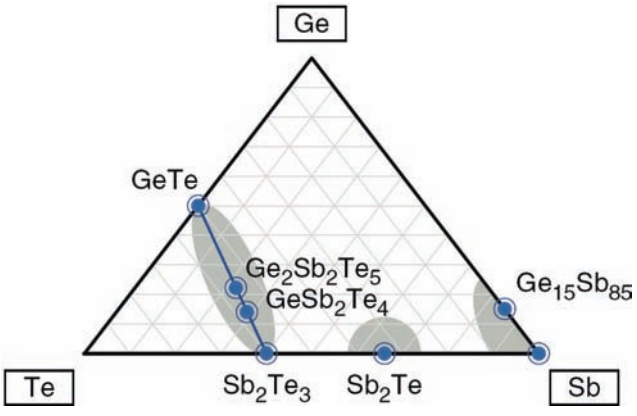

4. Structure and bonding in the crystalline and the amorphous phase

4.1. *Structure of crystalline phase*

The atomic arrangement in crystalline phase-change materials is characterized by a few typical structural motifs which can be linked to a unique bonding mechanism which prevails in the crystalline phase. Hence, the precise characterization of the atomic arrangement of the crystalline state can provide a valuable insight into the bonding of these materials and the resulting properties. We now turn to the discussion of typical crystal structures of phase-change materials, focusing on the well-known prototype materials on the pseudo-binary line between GeTe and Sb_2Te_3. The atomic structures of phase change materials exhibit generic features and structural motifs which are quite different from other materials that at first sight should behave similarly. This implies that phase change materials are characterized by a unique bonding mechanism which will be discussed later. The two limiting cases of the pseudo-binary line, GeTe and Sb_2Te_3, are well suited to discuss the structure and bonding mechanisms that rule phase-change materials. They are depicted in Figure 3.[22]

Meta-stable crystalline phase: A meta-stable crystalline phase is a crystalline phase whose formation is controlled by kinetics. Annealing a solid with a meta-stable crystalline phase can lead to a transformation to a lower-energy state crystalline phase.

Peierls instability: Consider a one-dimensional metal with an electron gas filling all conduction band orbitals out to the wavevector k_F, at absolute zero temperature. Peierls suggested that such a linear metal is unstable with respect to a static lattice deformation vector $G = 2K_F$. Such a deformation creates an energy gap at the Fermi surface, thereby lowering the energy of electrons and forming an energy gap.

Let us first consider GeTe. It exhibits a structure that closely resembles a rock-salt structure, with Ge occupying the cation and Te at the anion sublattice. At temperatures below approximately 700 K, atomic displacements deform this lattice. First, there is a relative shift of the two sublattices along the [111]-direction. This reduces the number of bonds from six to three short bonds (and three long bonds), in line with the *Peierls-model* of distortions for a system with an average number of three p-electrons.[23,24] As a secondary effect, the atomic displacements lead to a small decrease of the cell angle. Altogether, a rhombohedral rather than a cubic cell is obtained.[25] Above around 700 K, a second order phase transition lifts the distortion.

Not only the structure of GeTe, but also that of Sb_2Te_3 can be understood in terms of a distorted rock-salt-like structure. Again, there is an atomic alternation as antimony has only tellurium neighbours in an octahedral environment. However, since there is an excess of Te atoms, these would need to be arranged in neighbouring sites. Instead, well-separated layers, consisting of the sequence Te-Sb-Te-Sb-Te, form with interlayer bonding between adjacent Te planes being ascribed to Van der Waals interactions. For the following discussion, it will be instructive to view the space between the two layers as occupied by a layer of intrinsic vacancies. The layer periodicity depends on the Sb to Te-ratio as investigated by X-ray diffraction.[26]

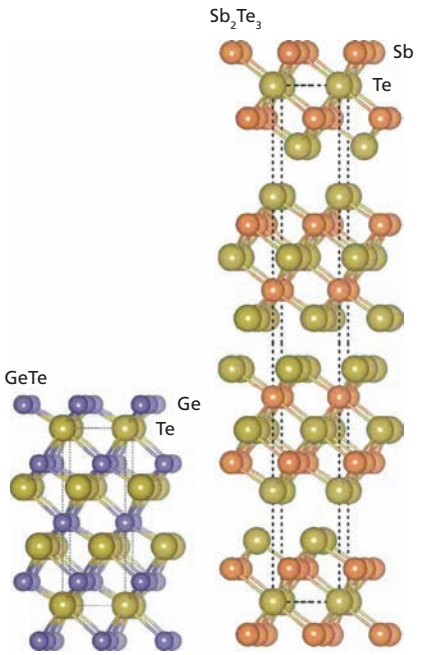

Figure 3: The crystal structures of GeTe and Sb_2Te_3 as explained in the text. Phase change materials inherit the principal structural features of these two limiting cases. Reproduced from ref.[22]

The Ge:Sb:Te-compounds inherit the aforementioned structural ingredients. In the *metastable crystalline phase*, they exhibit a rock-salt-like structure, with tellurium occupying the (formal) anion sublattice. The other cation sublattice is occupied by germanium, antimony and intrinsic vacancies. Thus, these metastable phases also feature an octahedral-like coordination. The atomic positions show (Peierls-like) distortions from the high-symmetry-positions. For compositions close to GeTe, also, a rhombohedral distortion of the unit cell is observed.[27] Interestingly, the occupation of the cation sublattice depends on the thermal history. After crystallization, typically, a random, chemically disordered occupation is obtained. Density functional theory calculations have been performed in order to find out whether there is an energetically preferred occupation.[22,28,29] The principal finding is that certain layer-sequences are favored, with the layers being orientated normal to the [111]-direction. The layer sequence is typically similar to what is found for Sb_2Te_3. The germanium-incorporation leads in most cases to the formation of additional -Te-Ge-Te-sequences within the layer. The initially randomly dispersed vacancies are shifted to form a vacant space between two layer-stacks. For $Ge_1Sb_2Te_4$, for instance, Da Silva et al.[22] obtain a Te-Sb-Te-Ge-Te-Sb-Te- sequence. Though an intermixing of Ge and Sb seems energetically not very different and has, in fact, been obtained for $Ge_2Sb_2Te_5$, here, Ge and Sb atoms do not populate separate but shared layers. This arises from the preference of Te-atoms to be surrounded by three Ge and Sb atoms. Without intermixing, the central Te-layer would be neighboured only by Ge-atoms. We note, however, that the same authors state that the theoretically most favourable structure is likely not obtained by experiment given the mismatch between optical properties calculated for those structures and the measured ones.[30] Very similar layer-sequences are obtained for stable, hexagonal phases as shown by Kooi and De Hosson.[31] Thus, it is reasonable to assume that the disordered metastable phase exhibits a tendency towards the same stacking sequence, but is kinetically hampered by slow atomic diffusion.[32]

4.2. *Optical Properties and the Origin of the Optical Contrast*

One of the unique properties that is employed in optical data storage is the change in optical properties upon crystallization. The optical properties, that

also probe the density of both occupied and unoccupied states, have been investigated experimentally[30,33] and theoretically.[34,35] In the visible range between approximately 1.5 and 3.1 eV, the dielectric function is governed by inter-band absorption. From an extrapolation of the measured spectra, it had been extrapolated that in comparison to the amorphous phase, the optical gap is typically smaller, with values of 0.2 to 0.6 eV for the crystalline phase. Hence, the gap falls below the typical lower boundary of the energy range that is accessible to *spectroscopic ellipsometry*. Recently, Welnic et al.,[34] have found a microscopic explanation for the pronounced optical contrast by employing time-dependent *DFT calculations*. They demonstrated that besides the decrease of the gap size, there is a pronounced change of the matrix elements for the optical transition from the valence to the conduction band upon crystallization. It is usually assumed that upon crystallization there is mainly a change in the joint density of states, but changes in the optical matrix elements are frequently ignored. Phase-change materials, however, differ significantly from the usual scenario. While this is an important insight, the computational complexity of these DFT calculations renders them of limited use for the development and optimization of new phase-change materials. This immediately raises the question of how novel phase-change materials can be identified and how such materials can be optimized efficiently.

Ellipsometry: Ellipsometry is an optical characterisation technique for the investigation of the dielectric properties such as complex refractive index or dielectric function of thin films.

DFT calculations: Density functional theory (DFT) is a quantum mechanical modelling method used in physics and chemistry to investigate the electronic structure of many-body systems, in particular atoms, molecules, and condensed phases.

Interestingly, the simplest scheme that we are aware of utilizes the optical properties of phase change materials in the infrared range. This is somewhat surprising, since in this frequency range, phase-change materials possess a broad transparency window. Nevertheless, the optical properties even below the absorption edge of crystalline and amorphous phase-change materials differ significantly.[36] This is shown in Figure 4a. The visual inspection of this figure reveals three differences between the spectra of the amorphous and the crystalline state of phase-change materials. The energy range where oscillations, which are indicative of the transparency of the phase change film, are observed, is larger for the amorphous state. This implies that the amorphous phase has a larger optical gap than the crystalline phase, confirming earlier extrapolations from optical spectroscopy data. In addition, even in the energy range below the bandgap, the crystalline films show absorption. This can be seen from the fact that the interference maxima are considerably below unity. Most likely this is due to some collective excitation of charge carriers. No such contribution is visible in the spectra of the amorphous phase. The most interesting difference, however, is the different spacing of the reflectance minima. Since, in this sample geometry, we are performing a simple interference measurement, the spacing of the reflectance minima is governed by the optical thickness, i.e., the product of the film thickness and the corresponding refractive index. The observation that the reflectance minima are much more closely spaced in the crystalline sample cannot be explained by the characteristic 5% decrease in film thickness upon crystallization, which would even lead to a corresponding increase in the spacing of the minima. Instead, the refractive index of the crystalline state has to be significantly higher than the refractive index of the amorphous phase. This distinctive difference can explain the pronounced optical contrast that characterizes phase-change materials. These observations are reflected by the dielectric functions fitted to these spectra.[36] Hence, these or similar measurements are ideally suited to identify and even optimize phase change materials.

A second example is shown in Figure 4b, which displays the reflectance spectra for $Ag_5In_5Sb_{60}Te_{30}$.[37] This material is frequently used in rewritable optical data storage as well. Again, a pronounced difference between the amorphous and crystalline state is found. In this case, the contribution of the free carriers is so pronounced that the oscillations are completely damped. A similar situation is also noticed in a phase change alloy such as InSbTe,[21] which possesses a highly conducting crystalline phase. Since so many different phase change materials show a pronounced change of their reflectance spectra in the infrared, a generic explanation is needed to account for this difference in the dielectric function of the two different states, and this will be discussed later.

FTIR spectroscopy: Infrared spectroscopy is a commonly used tool to gain information about the dielectric function of a material in the infrared region of the electromagnetic spectrum. A common laboratory instrument that uses this technique is a Fourier transform infrared (FTIR) spectrometer.

From the analysis of the *FTIR spectra*, we have concluded that the optical dielectric constant, which is closely related to electronic polarizability, is much larger in the crystalline state for all the phase change materials studied. This optical dielectric constant is derived from the dielectric function $\varepsilon(\omega)$ and includes all electronic contributions to this function but ignores a potential contribution from the orientation polarization and lattice distortions since the frequencies considered here are too high for those contributions to have any impact.

4.3. *Resonance bonding and a treasure map*

The data for the optical dielectric constant of the different amorphous phases can be explained quite well with a model that attributes one

Figure 4: (a) IR reflectance spectra of a $Ge_1Sb_2Te_4$ film. Blue, amorphous state; red, crystalline state. The solid lines describe the experimental data, while the dashes denote the simulation results. Upon crystallization, the thickness decreased from 1.13 to 1.03 μm (from Ref.[36]). (b) IR reflectance spectra of $Ag_5In_5Sb_{60}Te_{30}$ film. Blue, amorphous state; red, crystalline state. The solid lines describe the experimental data, while the dashed lines denote the simulation results. Upon crystallization, the thickness decreased from 0.94 to 0.88 μm. This phase change material does not display oscillations of the reflectance of the crystalline state since the absorption of the free carriers is more pronounced (from Ref.[37]).

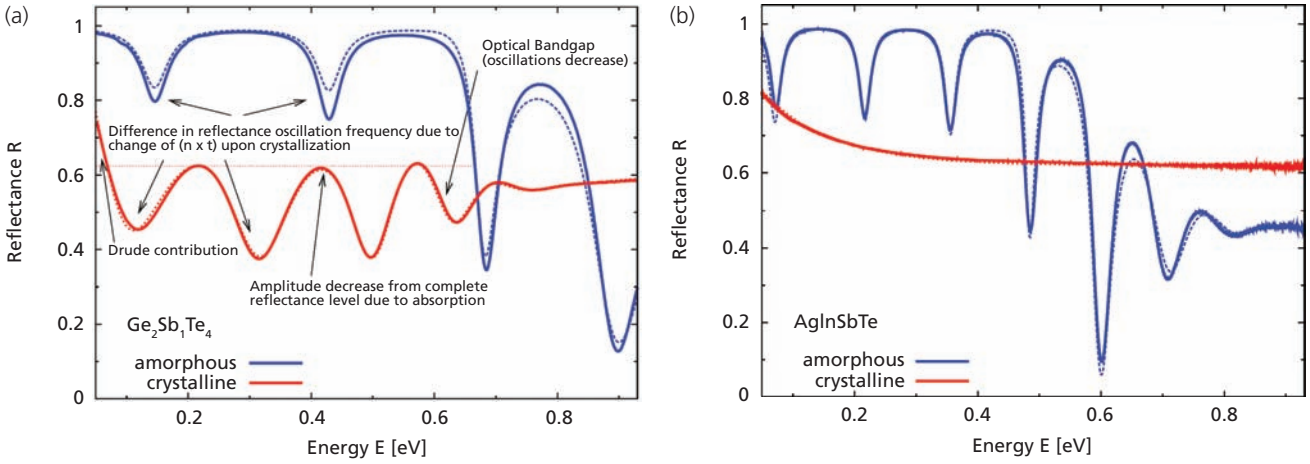

specific polarizability to each element contained in the corresponding phase change material.[36] This implies that all amorphous phase change materials behave in a similar fashion. Such a finding raises some doubts about whether an approach that assigns the unique properties of phase change materials to unique features of the amorphous state, such as the specific position of the Ge atoms, can successfully account for the unique properties of a wide range of phase change alloys. For the crystalline state, on the contrary, the optical dielectric constant could not be predicted based upon the density and stoichiometry of the material alone. This implies that there have to be changes of chemical bonding with stoichiometry for the crystalline state, which affect the optical dielectric constant.

Fortunately, the crystalline state has been extensively studied with techniques that enable the precise determination of the atomic positions, revealing structural features generic to all phase change materials. We can hence develop a simple model for the high optical dielectric constant (*electronic polarizability*) of crystalline phase change alloys. The simplest possible phase change material is elemental Sb. Indeed, recent work has shown that the ultra thin films of Sb display all the desirable properties of a non-volatile electronic memory.[38] Therefore, we can use this element to explain the unique properties of phase change materials. Figure 5 shows a simplified model of the atomic arrangement in Sb. Antimony has five valence electrons, 2 s-electrons and 3 p-electrons. Bonds to neighboring atoms are formed by the three p-electrons, since the energy difference between the s- and p-states is too high to allow the formation of an sp-hybrid. The atomic arrangement in pure Sb can be described to the first approximation as a simple cubic structure where every atom has six nearest neighbors. There are several degenerate electronic configurations consistent with this atomic arrangement. In this situation, the linear combination of the different electronic configurations can lower the energy of the structure. This is displayed in Figure 5. Here, a resonance bond is shown in the centre, which explains the high electronic polarizability of the crystalline phase change materials. The situation, in which a single, half filled p-band forms two bonds to the left and right (more than allowed by the 8-*N* rule), was called resonant bonding by Pauling.[39] The pronounced electron delocalization, which characterizes resonant bonding, leads to a significantly increased optical dielectric constant (electronic polarizability). This phenomenon is one of the fingerprints of resonance bonding.

Electronic polarizability: The total polarizability may usually be seperated into three parts namely electronic, ionic and dipolar. The electronic contribution arises from the displacement of the electron shell relative to a nucleus.

The true crystal structure of Sb is not a simple cubic structure, but an A7 structure, which can be described as a distorted simple cubic structure. This distortion increases electron localization since the two limiting electron configurations depicted in Figure 5 are no longer energetically equivalent. Thus, resonance bonding is weakened by the distortion, which is frequently termed a Peierls-like

Figure 5: A schematic viewgraph demonstrating the origin of resonance bonding for Sb. On the left-hand side, one limiting case for bonding in an undistorted Sb phase is depicted. The second limiting case is displayed on the right-hand side. The solid can minimize its energy by forming a hybrid wave function, which is sketched in the middle of this figure. This bonding is described as resonance bonding. The pronounced electron delocalization gives rise to an increased electronic polarizability (from Ref.[36]).

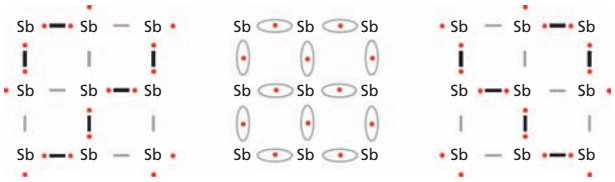

distortion. Hence, it is important to note that the distortion does not give rise to a large electronic polarizability and phase change behavior, but rather endangers it. The size of the contribution of resonance bonding can best be estimated from the relative increase of the electronic polarizability, i.e. $\frac{\varepsilon_{cryst}}{\varepsilon_{amo}} - 1$.

Resonance bonding is the cause of the large optical dielectric constant observed in all crystalline IV-VI compounds.[40] It results in larger optical dielectric constants than found in materials employing ordinary covalent bonding, because it gives smaller average band gaps (bonding–antibonding splitting) and larger optical matrix elements, as shown by Littlewood.[40] The crystal structures of phase change materials are all based on distorted cubic structures and all possess resonant bonding. This is, therefore, the cause of their higher optical dielectric constants. The existence of resonant bonding requires a longer-range order than the conventional electron pair bond of the *8-N rule*. An electron pair requires only the alignment of the electron orbitals which form the bond for its nearest neighbours. Resonant bonding, on the contrary, requires the second and higher neighbours to be aligned as well. In the amorphous state, this higher level of ordering is not possible, and so the structure reverts to a simple 8–*N* rule structure, which requires a lower level of ordering, as noted by Lucovsky and White.[41] This emphasizes that the bonding between the phases differs not only in coordination numbers as seen by *EXAFS* but also in their medium range order.

Thus, the decrease in ε_∞ values between the amorphous and crystal phases of phase change materials can be taken as clear evidence that the medium range order needed for resonant bonding is absent in their amorphous phases.[35] This change in bonding between the amorphous and crystalline phases, with a strong re-arrangement of the next nearest neighbours, is at least as significant as the lowering of the Ge coordination to four, or the formation of Ge-Ge bonds. This difference is more difficult to see in EXAFS.

For all amorphous phases, we observe very similar behavior for both PCMs as well as sp^3-bonded, tetrahedrally coordinated covalent semiconductors. However, only PCMs exhibit a significant increase in polarizability upon crystallization. This finding is attributed to a unique change of both structure and chemical bonding, giving rise to resonance bonding effects. Hence, from the viewpoint of property contrast it is not the amorphous phase but the crystalline phase, which is unique. The search for materials exhibiting the necessary optical contrast required for phase change memory applications can hence be redirected. Those compounds need to be identified which are prone to the occurrence of this particular flavour of covalent bonding. Since resonance bonding can only occur for semiconductors, which possess unsaturated covalent bonds, all sp^3-bonded materials can immediately be excluded.

In addition, materials, which rearrange to form saturated covalent bonds by pronounced local distortions, also will not possess resonance bonding. This tendency is directly related to the energetic difference between the outermost s- and p-electrons. A measure for this difference is the quantity

$$r_\pi^{-1} = [(r_p^A - r_s^A) + (r_p^B - r_s^B)]^{-1} \qquad (1)$$

where r_s^X and r_p^X denote the valence radii of the s- and p-orbital of atom X, respectively. The larger this quantity, the easier it is to form an sp- hybrid. Resonance bonding cannot prevail, when r_π^{-1} is large, since then the charge is localized between two atoms. Charge localization also characterizes ionic compounds, where the charge is located at the ion cores. Hence, ionic compounds also will not show resonance bonding. The tendency to form an ionic bond can be derived from a second quantity, i.e. r'_σ

$$r'_\sigma = r_p^A - r_p^B \qquad (2)$$

These two coordinates span the map for chalcogenides that was already developed for binary *chalcogenides* with an average number of valence electrons (N_{sp}) of 5 in the 1980s.[40] It has recently been extended to ternary chalcogenides, which leads to a map with many more compounds as displayed in Figure 6.[42] Using the radii given in Ref.[43], the resulting values for r'_s and r_π^{-1} are

8-N rule: The 8-N rule explains and predicts the atomic coordination in a wide range of materials composed of elements from the groups V, VI, VII. With N being the number of valence electrons of an atom, the rule states that the coordination of an atom in a covalent bonding configuration is equal to 8-N.

EXAFS: Extended X-ray Absorption Fine Structure utilises the details of how x-rays are absorbed by an atom in the vicinity of a core-level absorption edge. The variation in the absorption probability is a consequence of the local environment of the atom. EXAFS is especially sensitive to coordination chemistry, oxidation states, the type and distances of neighbour atom and the coordination number about the selected element.

Chalcogenides: A chalcogenide is a chemical compound consisting of at least one chalcogen (16th group elements namely S, Se, Te) element.

Figure 6: Map for numerous $N_p = 3$ systems. (a) A wide variety of materials is shown which differ in their tendency towards hybridization ('covalency'), r_π^{-1} and ionicity, r_σ^{-1}. Three types of systems are shown: group V elements (squares), binary $A^{IV}B^{VI}$ compounds (grey circles) and ternary alloys with different compositions including $A_2^{IV}B_2^{V}C_5^{VI}$ (triangles), $A^{IV}B_2^{V}C_4^{VI}$ (diamonds) and $A^{IV}B_2^{V}C_7^{VI}$ (pentagons). Bands of oxides, sulphides, selenides and tellurides are clearly discernible and are denoted by red, orange, yellow and blue letters to label the corresponding binaries. The insets on the left illustrate how the bonding mechanism varies with the coordinates. The starting point is a structure with predominant resonance bonding. The resonance character is weakened both by increasing hybridization as well as increasing ionicity. Increasing the former leads to larger distortions that favor a smaller number of more saturated covalent bonds. Increasing ionicity also reduces resonant bonding because now the charge is increasingly localized at the ion cores. Hence phase-change materials, marked by green circles, are all localized in a small region of the map. (b) A more detailed view of the small region in (a) in which the phase-change materials are localized. This region is characterized by the pronounced resonance bonding in the crystalline state (from Ref.[25]).

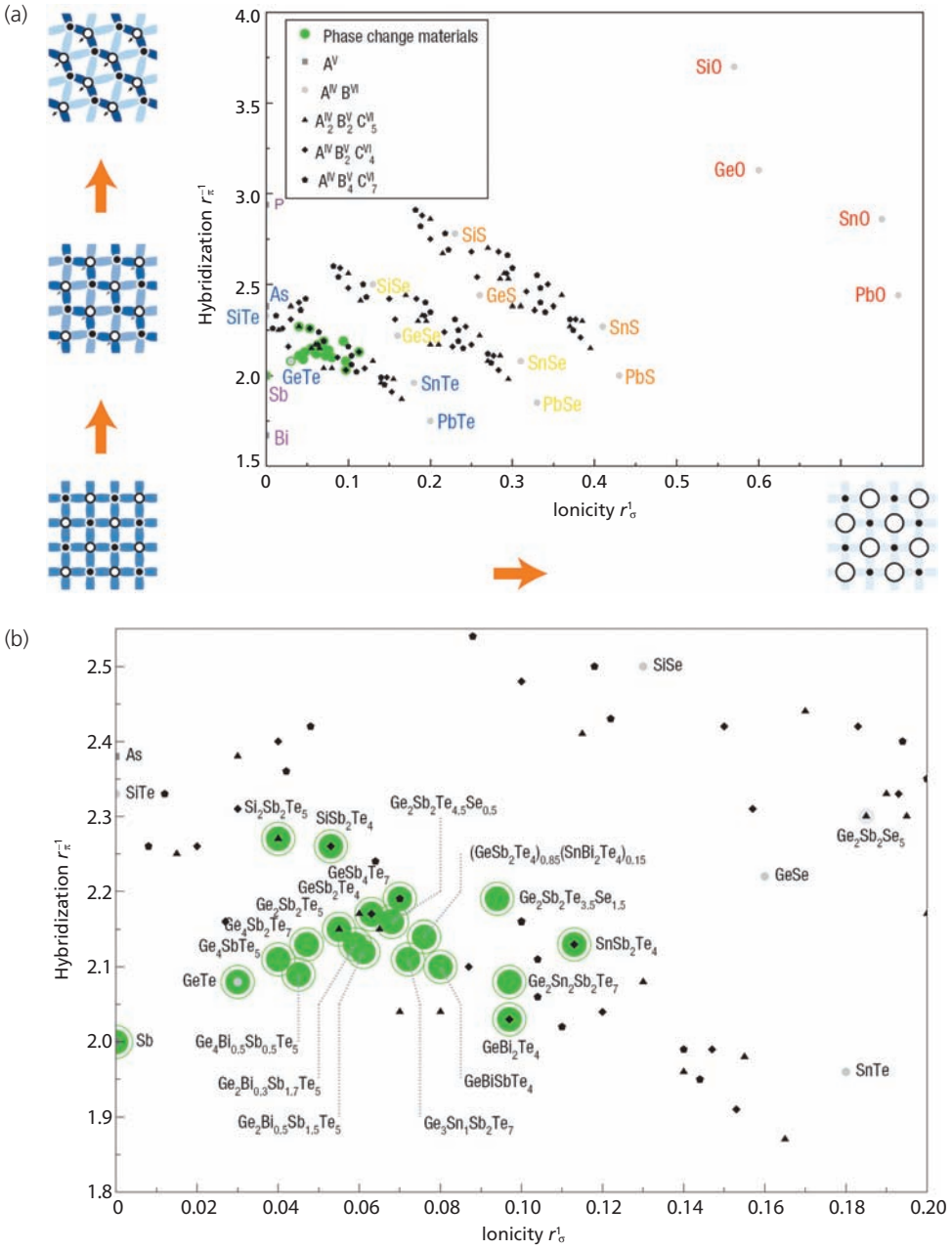

displayed in Figure 6a for a large number of suitable systems. More recently, the corresponding radii have also been obtained by density functional theory.[44,45] All systems displayed in Figure 6 have in common that they contain an average number of 3p-electrons per site and an about equal amount of formal anions and cations. It can be seen that sulphides, selenides and tellurides all form more or less separate bands. With the procedure outlined above various phase-change materials have also been inserted in Figure 6. Known phase-change alloys such as GeTe and materials consisting of (Si/Ge/Sn):(Sb/Bi):Te, e.g. the well-studied $Ge_1Sb_2Te_4$,[46] are all located in the same small region of the viewgraph. This implies that a unique range of hybridization and ionicity, limiting the number of materials that can sustain phase change properties, characterizes phase-change materials. More specifically, phase-change materials are found in an area of low ionicity and a limited degree of hybridization, which enables resonance bonding to prevail. The finding of resonance bonding in a limited region of the map can be understood, if we consider the schematic drawings at the border of Figure 6. These sketches denote how a perfect sixfold-coordinated system, which shows resonance bonding would be affected if either of the two coordinates increased. Increasing r_π^{-1} leads to a more pronounced formation of saturated covalent bonds and is accompanied by increasing distortions, since it invokes a departure from pure p-bonding. The increased charge localization diminishes resonance bonding and hence the electronic polarizability. The same happens if r'_σ increases and the charge is increasingly localized at the ion cores. Hence, it becomes obvious that resonant bonding can only be found in the region denoted by the filled green circles in Figure 6b. The map depicted therefore enables us to identify suitable candidates based only upon a material stoichiometry. This conclusion can even be exploited for material design, since the coordinates, which identify the bonding mechanism, are uniquely related to important material properties. At the same time, there are some device properties such as cyclability that cannot be predicted since for this important attribute of phase change memories also, the surrounding material plays an important role.

Future research may therefore attempt to transfer this scheme to other stoichiometries and other values of N_p. In that sense, the present two-dimensional map is only one projection plane within a higher-dimensional composition space. However it is a particularly important one, since it hosts typical phase-change materials including antimony, GeTe and the Ge:Sb:Te-class as well as materials derived by iso-electronic exchange. It has to be stressed that careful application of the map concept is advised. For instance, it is meaningless to put materials with an average number of p-electrons of two or four, or a pronounced deviation in composition from an equal amount of anions and cations such as e.g. $SnSe_2$, onto the same projection plane. Instead, a different projection plane should be chosen. Elements with d-states close to the *Fermi-level* are also not incorporated in the present scheme. So far, we have identified the unique structure and bonding in the crystalline state as well as the resulting properties (see ref.[47] for more detailed explanations).

Fermi-level: The highest occupied energy level in the ground state of a system of fermions.

5. Material Properties

5.1. *Electrical Properties*

In recent years, the electrical properties of phase-change materials have attracted considerable interest as research shifted from optical to electrical memories. Consequently, the conductivity in both the crystalline and the amorphous state, in particular, shall be reviewed here. The fact that it differs significantly between the two phases, as the exemplary measurement of the resistivity in Figure 7 shows, allows distinguishing between the different states. In $Ge_2Sb_2Te_5$, for instance, the specific electrical conductivity at room temperature changes upon crystallization from $\sim 4 \times 10^{-3}$ $\Omega^{-1}cm^{-1}$ to $\sim 1.5 \times 10^{+3}$ $\Omega^{-1}cm^{-1}$, that is by six orders of magnitude.[48] Further analysis shows that the concentration of charge carriers in the crystalline phase is particularly high, reaching values to the order of $\sim 1 \times 10^{20}$ cm^{-3}.[33] This is not a consequence of the small gap and thermal excitation, but is induced by a pronounced shift of the Fermi-level towards or even into the valence bands due to certain defects. In anticipation of the results presented in this section, this indicates that the states around the Fermi-level and their nature dominate the electrical behaviour of phase-change materials.

Furthermore, a recent investigation by Siegrist et al.,[49] successfully demonstrated a transition between thermally activated (non-metallic) and metallic transport in crystalline phase change materials such as $Ge_1Sb_4Te_7$, $Ge_1Sb_2Te_4$, $Ge_2Sb_2Te_5$, and $Ge_3Sb_2Te_6$ all of which lie on the GeTe-Sb_2Te_3 pseudo-binary line. This transition is mainly evidenced from the change in the sign of the temperature coefficient of the resistivity from non-metallic ($d\rho/dT < 0$) to metallic ($d\rho/dT > 0$) behaviour with increasing annealing temperature. The non-metallic behaviour has been attributed to a disorder-induced localization in the metastable

Figure 7: These are the phase transitions of a sample of $Ge_1Sb_2Te_4$ measured by the Van der Pauw-method. Crystallization occurs at around 420 K and leads to a significant drop in resistivity. A second irreversible, solid-solid transition is observed at about 600 K, which is identified as the transition from the metastable rocksalt- to the stable hexagonal phase. The charge transport in the amorphous phase is reasonably well described as thermally activated, while the crystalline phase obtained here exhibits a metal-like temperature-dependence (inset). (from Ref.[47])

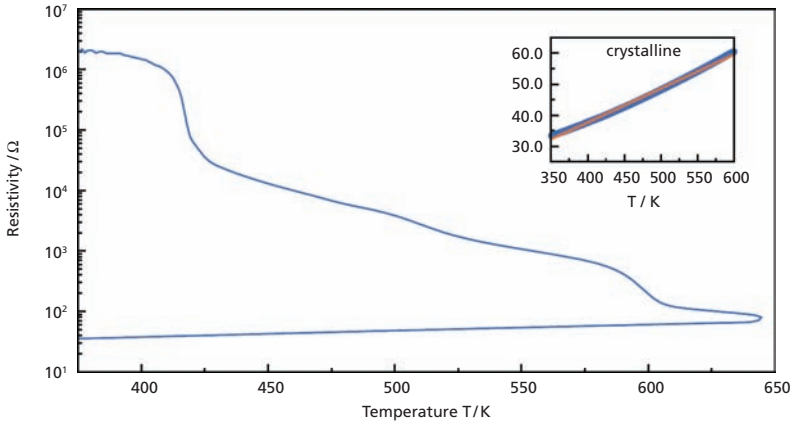

rock-salt-structure. At the transition to the metallic state, the corresponding electronic mean free path only amounts to 0.8 nm, which is interpreted as demonstrating a remarkably high level of atomic disorder. Furthermore, it has been suggested that controlling the degree of disorder in the crystalline state might enable the realization of multilevel resistance states which could be employed for high density electronic memories.[49]

5.2. *Current-voltage-characteristics and threshold switching in the amorphous phase*

One of the most active areas of research on phase-change materials is the investigation of the electrical conduction mechanism. Interest has been sparked not only by the need to precisely control this material property in devices but also due to the scientific richness of the topic. Unlike optical properties, electrical conductivity is very sensitive to all kinds of intrinsic and extrinsic parameters. It may, therefore, also serve as a probe of such parameters, though the results can be difficult to interpret given the variety of (possible) effects that have to be considered. As a basic result of frequently conducted thin film resistance measurements, the electrical conductivity for small electric fields exhibits thermally activated transport behaviour,

$$\sigma(T) = \sigma_0 \exp(-E_A^{cond.}/kT) \qquad (3)$$

with an activation energy of approximately half the measured optical gap, $E_A^{Cond.} \approx 1/2\ E_G^{opt.}$ The exponential temperature dependence that might appear as a challenge for applications does, in fact, not play a role. The contrast to the crystalline phase remains some orders of magnitude at all temperatures and is thus always sufficient to distinguish between the two states. Another fingerprint of the charge carriers and the mechanism of their transport are provided by Hall- and Seebeck measurements. From these measurements, the majority species of charge carrier transport can usually be deduced. However, respective measurements on Sb_2Te_3 and $Ge_2Sb_2Te_5$ by Baily and Emin[50] and Baily et al.[51] between 200 and 300 K yield opposite signs for both techniques. The Seebeck coefficient is large and indicates p-type conductivity. The Hall mobility is very low and anomalously signed (n-type). This is interpreted as an indication for conduction via the hopping of small polarons. Ielmini and Zhang[52] argued that trap limited transport is observed in phase-change materials. Such traps can be any kind of localized states close to extended states, arising, for instance, as band tails. In this picture, charge transport takes place within extended states, but the mobility is significantly reduced since unoccupied traps easily capture carriers. The physical model for this mechanism is *Poole-Frenkel conduction*. The litmus test of all models describing charge transport in amorphous phase-change materials, however, is whether they can account for the behaviour at elevated fields. The electrical conductivity of amorphous phase change materials exhibits a pronounced dependence on the strength of the applied electric

Poole-Frenkel conduction: The Poole-Frenkel conduction describes the dependency of field induced emission of free charge carriers released from trap states by taking into account the lowering of activation barrier by an electric field. If the concentration of trap states is low, the activation barrier lowering is proportional to the square root of the applied electric field.

field as shown in Figure 8. Two states can be discerned, the amorphous *OFF*- and *ON*-states. Until a critical field namely the threshold field E_t (or threshold voltage V_t) is reached, the system remains in the OFF-state. Here, the conductivity remains small, and follows first a linear, then an exponential and finally a super exponential path. When the field exceeds the threshold value, the conductivity largely increases. In this ON-state, the conductivity shows a linear field-dependence. From a technical point of view, this behaviour is very desirable since the crystallization of an amorphous bit is facilitated via Joule-heating. Without threshold switching, large voltages would need to be applied in order to drive a sufficiently large current for heating and thus crystallization to occur. Furthermore, threshold switching can be exploited for selector devices in electrical memories (as will be discussed later). Threshold switching is to be distinguished from memory switching which refers to crystallization, while threshold switching is a phenomenon specific to the amorphous phase and does not involve a structural phase transition. Experimentally, only applied voltages rather than fields can be measured, so studies on threshold fields employing electric testers have concentrated on the determination of voltages. If the geometry of the amorphous volume is known as in the as-deposited amorphous phase, the material-dependent field can be calculated from the voltage. It is typically about some tens of volts per micrometer.[10,53,54] This enables threshold switching and thereby the operation of phase-change devices at voltages as small as about 1 V for phase-change cells with a distance between the electrical contacts of about 100 nm (ignoring voltage drops at the interface to the electrodes). Sophisticated experiments have been designed to probe various aspects of threshold switching. Three of the key characteristics are here summarized. 1. Threshold switching occurs upon reaching the critical field strength only after a time delay. 2. After the threshold switch, the ON-state is retained unless the field strength drops below the holding field strength E_h.[8] Shortly after the ON-to-OFF transition, an electric field E with $E_h < E < E_t$ is sufficient to recover the ON-state. Most authors suppose that threshold switching is an electronic (rather than a thermal or structural) effect.[10] Emin[55] concludes that at elevated fields, the density of small polarons becomes larger. Thus, due to their proximity, lattice deformations become unfeasible once the threshold field is reached. Therefore, carriers may not localize anymore and the material becomes highly conductive. In the picture of Ielmini and Zhang,[56] Ielmini[57] (and references therein), that is Poole-Frenkel conduction, the electric field increases the probability of a carrier that occupies one trap to get to another one nearby. At low fields, this

Figure 8: The current–voltage characteristics of phase-change materials (device under test, DUT), shown schematically in both linear (left) and logarithmic scaling (right), exhibit an interesting effect called threshold switching. For small electric fields, the curves of the low resistive, crystalline and the high resistive, amorphous phase differ significantly. However, the situation changes if a critical voltage (corresponding to a field strength of some ten V/μm) is exceeded. The amorphous phase suddenly becomes much more conductive, switching to the so-called ON-state as opposed to the OFF-state. This effect, called threshold switching, enables sufficient joule heating for crystallization (memory switching) at moderate voltages. Further aspects of threshold switching marked in the graphs are discussed in the text (Reproduced from ref.[47]).

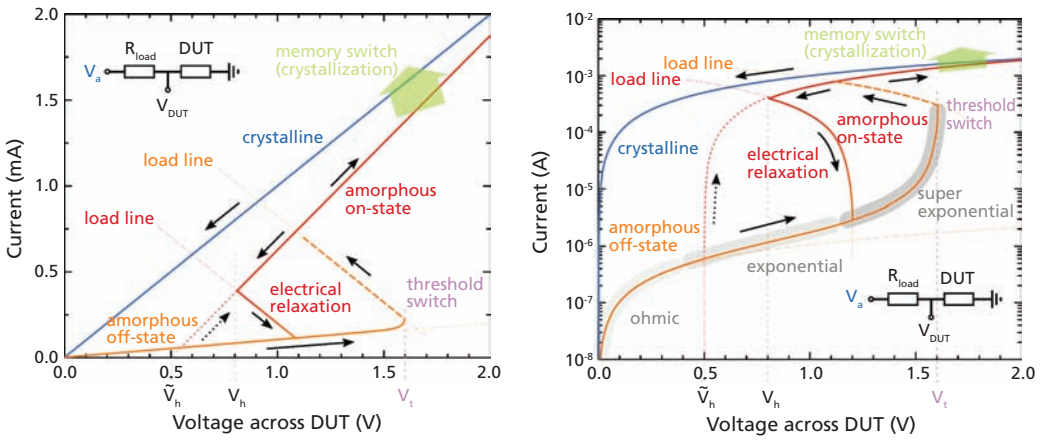

requires extended states. At the threshold field, however, direct tunnelling also becomes possible, leading to a conductivity increase. Another model presumes that threshold switching stems from a field-and carrier density-dependent generation mechanism, thus providing positive feedback once a critical field is attained. At low fields, however, recombination counterbalances generation.[10,58,59] There are various possible microscopic models that could account for this phenomenological effect such as impact ionization.[60] An alternative to the electronic models of threshold switching is provided by field-induced nucleation.[61] It is argued that at the threshold field, a crystalline filament forms in the amorphous volume and connects the electrodes. The origin of this effect is ascribed to the field-dependence of the free energy of the system. Depending on the size of the filament, it is either stable or collapses upon removing the external potential.

5.3. *Crystallization kinetics*

The time-limiting step in applications of phase-change materials is the crystallization process. A number of strategies have been developed to identify materials with particularly rapid crystallization kinetics.

Figure 9: (a) Growth-dominated recrystallization indicates the growth of the crystalline region from the crystalline rim. (b) Nucleation-dominated recrystallization is employed if the number of crystalline nuclei grows (from Ref.[63]).

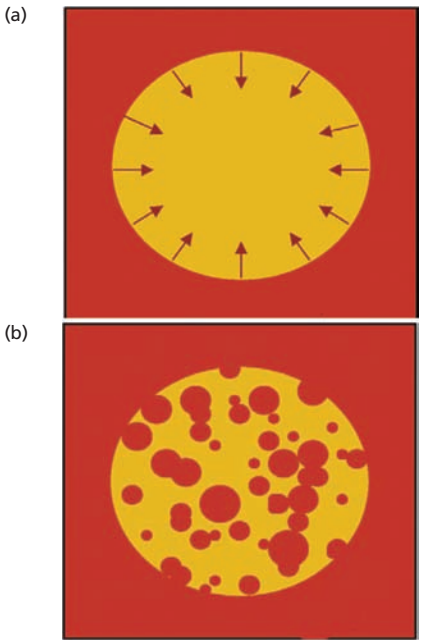

A systematic study performed by Coombs et al.[62] has proved to be particularly useful. It demonstrated that two different classes of phase change materials can be defined: nucleation- and growth-dominated materials. The difference between these two material classes is depicted in Figure 9.[63] This figure shows the two different mechanisms that are typically observed in phase change materials when an amorphous region is recrystallized under the influence of a laser beam or a current pulse, i.e. in optical or electronic data storage. In nucleation-dominated materials, the increase of temperature upon, for example, the application of a laser pulse, leads to the formation of crystalline nuclei that subsequently grow in the amorphous region. For growth-dominated materials on the other hand, an increase in temperature is accompanied by the growth of crystalline regions from the crystalline rim surrounding the amorphous area. In this case, no new crystalline nuclei are formed.

Various attempts to understand the microscopic basis of rapid crystallization kinetics in phase-change materials have been reported. These include a study of the correlation between vacancies and the observed speed of recrystallization,[64] and systematic studies of the recrystallization along the pseudobinary line between GeTe and Sb_2Te_3.[16] Several approaches have also focused on determining atomic positions in the amorphous and crystalline states.[65,66] Clearly, it would be a breakthrough, if the correlation between atomic structure, material properties, and crystallization kinetics could be derived from a microscopic understanding. At the same time, a knowledge of atomic positions for the amorphous and crystalline states does not yet provide the necessary activation barriers to describe the speed of crystallization. Hence, many experimental studies have focused on the determination of activation barriers for the overall crystallization process, often using a concept developed by Johnson, Mehl, and Avrami.[67,68]

More recently, investigations have successfully separated the contributions of nucleation and crystal growth that govern crystallization. These studies have been facilitated by the pronounced density change between the amorphous and crystalline phases, which is usually somewhere between 5% and 10%.[69] Hence, atomic force microscopy can be employed to determine the formation of crystalline nuclei in an amorphous matrix.[70,71] From such experiments, the dependence of nucleation rate and growth velocity on temperature has been determined for various alloys.[71] Interestingly, the growth velocity of the different alloys studied shows systematic trends for different stoichiometries.

In particular, the activation energy for crystal growth increases with Ge content. More importantly, more pronounced variations of nucleation rates with film stoichiometry have been reported. These differences have motivated a study of the undercooling of encapsulated liquid phase change droplets.[72] From these experiments, the interfacial energy between the liquid and the crystalline states for different phase change alloys has been derived. The interfacial energy is not only found to be surprisingly low, which can explain the easy formation of crystalline nuclei,[72] but it also shows systematic trends upon changing stoichiometry. In particular, materials with a smaller interfacial energy show nucleation-dominated crystallization, while those materials with a higher interfacial energy show growth-dominated crystallization. This finding implies that materials for which growth-dominated crystallization prevail are simply characterized by slow nucleation (see ref.[63]).

Super-RENS: Optical data storage is usually diffraction limited, i.e. the smallest possible structures that can be stored and retrieved are defined by the laser wavelength of the storage device and the aperture of the lens in the recorder (far-field condition). However, in near-field the diffraction limit can be circumvented, employing the Super-RENS (Super REsolution Near field Structure) effect.

6. Applications and Outlook

This section provides an overview of various applications that employ phase-change materials in the field of data storage, and their scope for future development.

6.1. *Optical Storage*

Optical data storage devices represent the most common application of phase-change based recording. The past decades have shown recording density increased by roughly a factor of hundred and the data-transfer rate by a factor of thousand. This is achieved mainly by reducing the wavelength of the laser used, from infrared to red and to blue-violet, and increasing the numerical aperture of the lens used, from 0.5 to 0.6 and then to 0.85.[1] With the introduction of blue laser light and maximization of the numerical aperture, the race for higher resolution and hence the development of this field may at first seem to be exhausted. Room for increasing storage capacity would be left only by increasing the number of data layers per disk. At present, a 100 GB disk employing three data layers marks the upper limit for such data storage devices, paving the way to a fourth generation of commercial optical phase-change based media.[73] However, another way of increasing capacity has been found in the course of phase-change research which is near-field recording. Here, an optical element is placed close to the surface of the medium, at a distance that is much smaller than the optical wavelength. This allows employing evanescent waves to manipulate bits on the medium beyond the diffraction limit.[74] The so-called super-RENS effect (super-resolution near-field structure) refers to the observation that structures smaller than the optical wavelength can be obtained by combining phase-change films with an additional thin layer in an optical near-field range.[75] In other words, the part of the optical system that needs to be located very close to the phase-change film to enable near-field recording is incorporated into the disk structure itself. The extra layer typically functions as a dynamic aperture, which should at the same time be small and highly transmittive (aperture-type *Super-RENS*). Materials successfully employed for these mask layers typically comprise materials related to phase-change materials such as antimony,[76] Sb_2Te_3,[77] and PbTe[78] or even phase-change materials themselves.[79]

It is clear that laser illumination-or more precisely its intensity profile-must cause an optical nonlinear response in the mask layer. The effect of super-resolution may be achieved by various types of interaction between matter and light. No consensus on the exact origin of the super-RENS effect using the aforementioned materials has been reached yet. Mostly, a predominantly thermal effect is considered. Laser irradiation leads to heating of the resolution-enhancing layer. Since the optical properties of the mask layer material are temperature-dependent (thermo reflectance), an aperture is created.[80] If even melting occurs at the center of the laser spot (given sufficient laser power is provided), the locally confined change in optical properties is even more pronounced. As a means to gain information on the structure and temperature of the respective portions of the mask layer, Raman scattering has been suggested.[81] Li et al.[82] proposed thermal expansion and the consequent change in light transmission as a possible origin for the super-resolution effect. Tominaga et al.,[83] argued that super-RENS might stem from a ferroelectric catastrophe in the mask materials. Other authors consider a predominance of electronic effects such as saturable absorption due to band filling by free carriers.[79] Liu and Wei[84] state that the optical non-linear absorption characteristics (here of AIST) lead to recording beyond the diffraction limit. Thus, given the variety of proposed explanations but also the potential benefit, the field of phase change based near-field recording remains a potentially rewarding research area (see ref.[47] for more detailed explanations).

6.2. *Electronic Storage*

Reversible resistance states in phase-change materials were introduced in 1968 by Ovshinsky.[8] This investigation initiated a first wave of studies with the aim of creating an electronic memory. Nevertheless, only now due to the availability of

Figure 10: Cell resistance after application of set pulses with different amplitude and length, each starting from the amorphous reset state. The colour of each data point represents the cell resistance after the test pulse. For pulses longer than 4 ns a broad crystallization window opens between 1.0 and 1.5 V (from Ref.[5]).

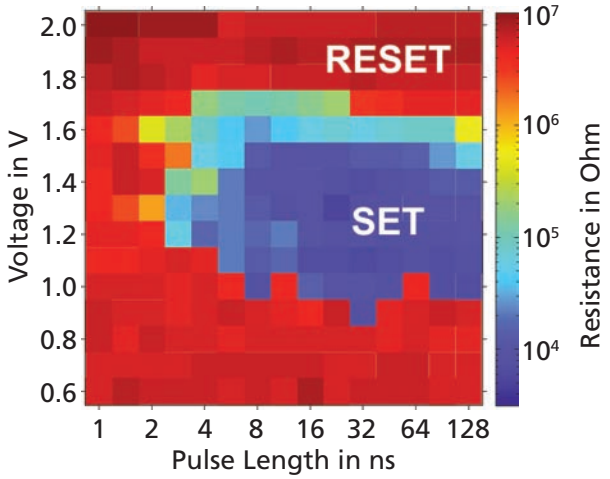

fast switching phase change materials and the ability to create nanoscale structures, it is possible to create competitive, non-volatile phase change based electronic memories: phase change random access memory, usually abbreviated PRAM or PCRAM. As can be seen from the *PTE-diagram* shown in Figure 10, operation can proceed on the timescale of few nanoseconds which is orders of magnitude faster than Flash. This puts PCRAM in the position of a universal memory that combines the best of both DRAM and Flash.[53,85] Moreover, the attainable sub-25 nm size scalability, 10 ns read/write speeds, 10^8 cyclablity surpass even the existing memories, while having low power consumption and radiation hardness. Hence, it is not surprising that the development of such memory cells has benefited from many industrial contributions.

Recently, an improved version of a *PCRAM-cell*, the so-called stackable cross-point memory has been developed that integrates the cell selector into the cell design as shown in Figure 11.[86] By the use of an *Ovonic threshold switch* (OTS), a selector with no more than the same spatial footprint as the memory cell itself is possible. This is to be contrasted with other, spatially more demanding designs mentioned in the recent review of Burr et al.[4] The OTS is just a thin layer of a material that exhibits threshold switching. If the voltage drop over the OTS due to the voltage applied between the word and bit line exceeds its threshold field, the memory cell that is in series with the OTS is selected. The simple design may also allow the stacking of layers of PCRAM-cells, and increase the storage density by making use of the third dimension as shown in figure 11. PCRAM makes extensive use of the threshold switching effect presented above to supply sufficient Joule heating power to quickly raise the temperature to levels high enough for crystallization to occur on a short timescale (cf. Figure 8). Very high voltages would be required, if threshold switching did not occur. Thus, PCRAM avoids voltage upconversion and the problems linked with high voltages in nanoscale above-electronics. Production schemes for PCRAMs involve the development

PCRAM: Phase Change Random Access Memory (PCRAM or PRAM) is one of the emerging non-volatile memory technologies, exploiting the unique behaviour of change in the resistance of nearly three orders of magnitude between amorphous and crystalline phases of chalcogenide based phase change materials.

Ovonic threshold switch: Threshold switching in chalcogenide materials is known to occur when an appropriate electric field is applied, the device switches from high resistance off state to low resistance conducting state. Upon removal of the applied electric field, when the current/voltage falls below a holding value, the device reverts back to the initial high resistance state forming an Ovonic threshold switch.

PTE-diagram: The power-time-effect (PTE) diagram reveals an in-situ measurement of the change in reflectivity/resistivity with respect to the applied power (optical/electrical) and time.

Figure 11: (left) An SEM cross section of a single cell structure consist of PCM layers as a storage element and an OTS layer as a selector in a stackable cross-point memory device. (right) The SEM cross section shows a vertically integrated, stackable cross-point memory device, compatible with mainstream CMOS technology, which employs an area-efficient structure (from Ref.[86]).

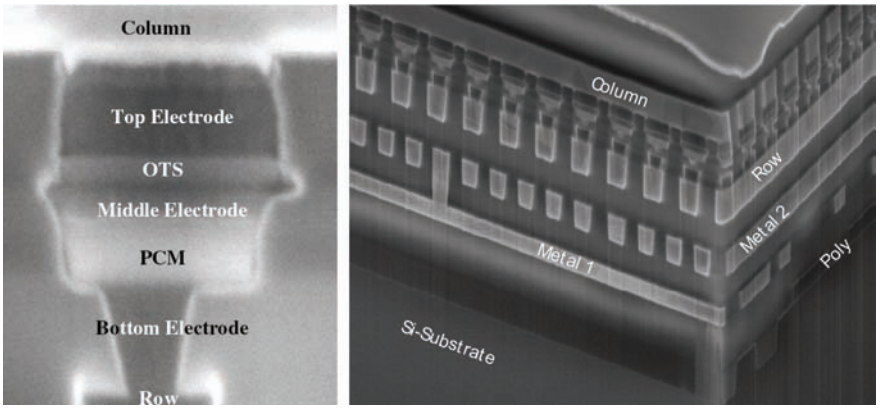

of techniques besides sputtering that allow for effective cell fabrication. For instance, large aspect ratios require techniques such as atomic layer deposition.[87] So far, the preparation techniques reported include chemical vapor deposition,[88] evaporation,[89] electro deposition,[90] pulsed laser deposition,[91] and solution-phase deposition.[92]

Among the criteria for a memory technique to be promising, scalability is a key requirement. It should be possible to exploit the steady improvement in reducing feature sizes in mass production to enable increasing data densities. A lack of scalability is one of the reasons why alternatives to Flash memory are actively pursued. Two factors may be discerned when scalability is addressed. On the one hand, the phase-change material must retain its properties despite a reduction in its volume. On the other hand, the space taken up by dielectrics and the electronics necessary to address and control the memory cell must also be taken into account. Nano-scaling is particularly advantageous to phase-change memory, since both energy consumption and crystallization time decrease with cell volume. The latter stems from the fact that with the decreasing size of memory cells, growth becomes the more prominent re-crystallization mechanism. The impact of nano-scaling on the material and device characteristics has recently been summarized in detail in the work of Raoux et al.[93] So far, we have described the advantages of PCRAM over competing memory technologies in terms of its non-volatility, speed and attainable storage density. Another aspect, however, is cyclability (i.e., the number of possible write-cycles). The two main wear processes identified so far are electro-migration and void formation. It is found that for cells based on Ge:Sb:Te materials, the spatial distribution of the elements changes upon multiple set and reset operations. In particular, antimony accumulates at the cathode, pushing germanium aside. Thus, the composition in the active volume and thereby the cell properties change. Operation at reversed polarity, though, can "repair" such a cell. The density change upon crystallization and atomic mobility may also hamper electrical contact via void formation.[94] In addition, degradation of the electrodes (e.g., diffusion into the phase-change material) and phase segregation in the case of non-stoichiometric materials may also be regarded as limiting factors. Nevertheless, though the exact number of possible cycles depends on a variety of factors, it has been proven to exceed the corresponding value of Flash by several orders of magnitude.[95]

Acknowledgements

The data presented summarize previous theoretical investigations and experimental studies, including two recent reviews [ref. 47 and 63]. Hence we would like to thank all past and present members of the phase change group; in particular D. Lencer, M. Salinga, and W. Welnic, are gratefully acknowledged. One of the authors, M.A thanks the Alexander von Humboldt foundation for the Post Doctoral research fellowship.

Received 17 May 2011.

References

1. Wuttig, M.; Yamada, N. *Nature Mater.* 2007, 6, 824.
2. Meinders, E. R.; Mijritskii, A. V.; van Pieterson, L.; Wuttig, M. *Optical Data Storage: Phase Change Media and Recording* (Springer, Berlin, 2006).
3. Roux, S.; et al. *IBM. J. Res. & dev.* 2008, 52, 465.
4. Burr, G. W.; et al. *J. Vacuum Sci. Technol. B* 2010, 28, 223.
5. Bruns, G.; et al. *Appl. Phys. Lett.*, 2009, 95, 043108.
6. Lencer, D. *Doctoral thesis*, RWTH Aachen University, 2010.
7. Micoulaut, M.; Raty, J. Y.; Otjacques, C.; Bichara, C. *Phys. Rev. B* 2010, 81, 174206.
8. Ovshinsky, S. R. *Phys. Rev. Lett.* 1968, 21, 1450.
9. Adler, D.; Henisch H. K.; Mott, N.F. *Rev. Mod. Phys.* 1978, 50, 209.
10. Adler, D.; Shur, M. S.; Silver, M.; Ovshinsky, S. R. *J. Appl. Phys.* 1980, 51, 3289.
11. Feinleib, J.; deNeufville, J.; Moss, S. C.; Ovshinsky, S. R. *Appl. Phys. Lett.* 1971, 18, 254.
12. Chen, M.; Rubin, K. A.; Barton, R. W. *Appl. Phys. Lett.* 1986, 49, 502.
13. Yamada, N.; Takenaga, M.; Takao, M. *Proc. SPIE* 1986, 695, 79.
14. Ohno, E.; Yamada, N.; Kurumizawa, T.; Kimura, K.; Takao, M. *Jpn. J. Appl. Phys.* 1989, 28, 1235.
15. Yamada, N; et al. *Jpn. J. Appl. Phys.* 1987, 26, 61.
16. Yamada, N.; Ohno, E.; Nishiuchi, K.; Akahira, N.; Takao, M. *J. Appl. Phys.* 1991, 69, 2849.
17. Kalb, J.; Spaepen, F.; Wuttig, M. *J. Appl. Phys.* 2005, 98, 054910.
18. Lankhorst, M. H. R.; et al. *Jpn. J. Appl. Phys.* 2003, 42, 863.
19. Solis, J.; Afonso, C. N.; Trull, J. F.; Morilla, M. C.; *J. Appl. Phys.* 1994, 75, 7788.
20. Pieterson, L. van.; Schijndel, M. van.; Rijpers, J. C. N.; Kaiser, M. *Appl. Phys. Lett.* 2003, 83, 1373.
21. Anbarasu, M.; Rausch, P.; Zalden, P.; Volker, H.; Raty, J.; Bichara, C.; Mazzarello R.; Wuttig, M. (unpublished)
22. Da Silva, J. L. F.; Walsh, A.; Lee, H. L. *Phys. Rev. B* 2008, 78, 224111.
23. Gaspard, J. P.; Pellegatti, A.; Marinelli, F.; C. Bichara, *Phil. Mag. B* 1998, 77, 727.
24. Littlewood, P. B. *CRC Critical Rev. Solid State Mater. Sci.* 1984, 11, 229.
25. Lencer, D.; Salinga, M.; Grabowski, B.; Hickel, T.; Neugebauer, J.; Wuttig, M. *Nature. Mater.* 2008, 7, 972.
26. Kifune, K.; Kubota, Y.; Matsunaga, T.; Yamada, N. *Acta Crystallogr. Sect. B* 2005, 61, 492.
27. Matsunaga, T.; et al. *J. Appl. Phys.* 2008, 103, 093511.
28. Sun, Z. M.; Zhou, J.; Ahuja, R. *Phys. Rev. Lett.* 2006, 96, 055507.
29. Sun, Z.; et al. *Solid State Commun.* 2007, 143, 240.
30. Park, J. W.; et al. *Phys. Rev. B* 2009, 80, 115209.
31. Kooi, B. J.; De Hosson, J. T. M. *J. Appl. Phys.* 2002, 92, 3584.
32. Matsunaga, T.; Yamada, N. *Phys. Rev. B* 2004, 69, 104111.
33. Lee, B. S.; Abelson, J. R.; Bishop, S. G.; Kang, D. H.; Cheong, B. K.; Kim, K. B. *J. Appl. Phys.* 2005, 97, 093509.
34. Welnic, W.; Botti, S.; Reining, L.; Wuttig, M.; *Phys. Rev. Lett.* 2007, 98, 236403.

35. Huang, B.; Robertson, J. *Phys. Rev. B* 2010, 81, 081204.
36. Shportko, K.; Kremers, S.; Woda, M.; Lencer, D.; Robertson, J.; Wuttig, M. *Nature Mater.* 2008, 7, 653.
37. Wuttig, M. *Phys. Status Solidi B*, 2009, 246, 1820.
38. Raoux S.; Wuttig, M. *Phase Change Materials: Science and Applications* (Springer, New York, 2009).
39. Pauling, L. *Nature of Chemical Bond* (Cornell University Press, Ithaca, New York, 1939).
40. Littlewood, P. B. *J. Phys. C: Solid State Phys.* 1980, 13, 4855.
41. Lucovsky G.; White, R. M. *Phys. Rev. B* 1973, 8, 660.
42. Lencer, D.; et al. *Nature Mater.* 2008, 7, 972.
43. Chelikowsky, J. R.; Philips, J. C. *Phys. Rev. B* 1978, 17, 2453.
44. Zhang, S. B.; Cohen, M. L. *Phys. Rev. B* 1989, 39, 1077.
45. Mann, J. B. Los Alamos Science Report. 1968, LA 3691.
46. Matsunaga, T.; Yamada, N. *Phys. Rev. B* 2004, 69, 104111.
47. Lencer, D; Salinga, M; Wuttig, M. *Adv. Mater.* 2011, 23, 2030.
48. Friedrich, I.; Weidenhof, V.; Njoroge, W.; Franz, P.; Wuttig, M. *J. Appl. Phys.* 2000, 87, 4130.
49. Siegrist, T; et al. *Nature Mater.* 2011, 10, 202.
50. Baily, S. A.; Emin, D. *Phys. Rev. B* 2006,73, 165211.
51. Baily, S. A.; Emin, D.; Li, H. *Solid State Commun.* 2006, 139,161.
52. Ielmini, D.; Zhang, Y. G. *Appl. Phys. Lett.* 2007, 90, 19 2102.
53. Lankhorst, M. H. R.; Ketelaars, B. W. S. M. M.; Wolters, R. A. M. *Nature Mater.* 2005, 4, 347.
54. Krebs, D.; Raoux, S.; Rettner, C. T.; Burr, G. W.; Salinga, M.; Wuttig, M. *Appl. Phys. Lett.* 2009, 95, 082101.
55. Emin, D. *Phys. Rev. B* 2006, 74, 035206.
56. Ielmini, D.; Zhang, Y. G. *J. Appl. Phys.* 2007, 102, 054517.
57. Ielmini, D. *Phys. Rev. B* 2008, 78, 035308.
58. Pirovano, A.; Lacaita, A. L.; Benvenuti, A.; Pellizzer, F.; Bez, R. *IEEE Trans. Electron Devices* 2004, 51, 452.
59. Redaelli, A.; Pirovano, A.; Benvenuti, A.; Lacaita, A. L. *J. Appl. Phys.* 2008, 103, 111101.
60. Jandieri, K.; Rubel, O.; Baranovskii, S. D.; Reznik, A.; Rowlands, J. A.; Kasap, S. O. *J. Mater. Sci.: Mater. Electron.* 2009, 20, 221.
61. Karpov, V. G.; Kryukov, Y. A.; Savransky, S. D.; Karpov, I. V. *Appl. Phys. Lett.* 2007, 90, 123504.
62. Coombs, J. H.; et al., *J. Appl. Phys.* 1995, 78, 4918.
63. Welnic, W.; Wuttig, *M. Materials today* 2008, 11, 20.
64. Matsunaga, T.; Yamada, N. *Jpn. J. Appl. Phys.* 2002, 41, 1674.
65. Kolobov, A. V.; et al., *Nature Mater.* 2004, 3, 703.
66. Baker, D. A.; et al., *Phys. Rev. Lett.* 2006, 96, 255501.
67. Johnson, W.; Mehl, R. *Trans. AIME* 1939, 135, 416.
68. Avrami, M. J. *Chem. Phys.* 1939, 7, 1103.
69. Njoroge, W. K.; et al. *J. Vac. Sci. Technol.* A 2002, 20, 230.
70. Weidenhof, V.; et al. *J. Appl. Phys.* 1999, 86, 5879.
71. Kalb, J.; et al. *Appl. Phys. Lett.* 2004, 84, 5240.
72. Kalb, J.; et al. *J. Appl. Phys.* 2005, 98, 054910.
73. Yamada, N.; Kojima, R.; Nishihara, T.; Tsuchino, A.; Tomekawa, Y.; Kusada, H. *European Phase-Change and Ovonics Symposium* 2009.
74. Betzig, E.; Trautman, J. K. *Science* 1992, 257, 189.
75. Tominaga, J.; Nakano, T.; Atoda, N. *Appl. Phys. Lett.* 1998, 73, 2078.
76. Fukaya, T.; Tominaga, J.; Nakano, T.; Atoda, N. *Appl. Phys. Lett.* 1999, 75, 3114.
77. Shi, L. P.; Chong, T. C.; Hu, X.; Li, J. M.; Miao, X. S. *Jpn. J. Appl. Phys.* 2006, 45, 1385.
78. Lee, H. S.; et al. *Appl. Phys. Lett.* 2004, 85, 2782.
79. Lee, H. S.; et al. *Appl. Phys. Lett.* 2008, 93, 221108.
80. Kuwahara, M.; Shima, T.; Fons, P.; Fukaya, T.; Tominaga, J. *J. Appl. Phys.* 2006, 100, 043106.
81. Kuwahara, M.; Shima, T.; Fons, P.; Tominaga, *J. Appl. Phys. Expr.* 2009, 2, 082402.
82. Li, J. M.; et al. *Jpn. J. Appl. Phys.* 2007, 46, 4148.
83. Tominaga, J.; Shima, T.; Kuwahara, M.; Fukaya, T.; Kolobov, A.; Nakano, T. *Nanotechnology* 2004, 15, 411.
84. Liu, J.; Wei, J. S.; *J. Appl. Phys.* 2009, 106, 083112.
85. Wuttig, M. *Nature Mater.* 2005, 4, 265.
86. Kau, D.; et al. *Electron Devices Meeting (IEDM)*, 2009, 617.
87. Ritala, M.; et al. *Microelectron. Eng.* 2009, 86, 1946.
88. Kim, R. Y.; Kim, H. G.; Yoon, S. G. *Integrated Ferroelectrics* 2007, 90, 80.
89. Wagner, T.; Orava, J.; Prikryl, J.; Kohoutek, T.; Bartos, M.; Frumar, M. *Thin Solid Films* 2009, 517, 4694.
90. Leimkuhler, G.; Kerkamm, I.; Reineke-Koch, R. *J. Electrochem. Soc.* 2002, 149, C474.
91. Nazabal, V.; et al. *Appl. Opt.* 2008, 47, C114.
92. Mitzi, D. B.; Raoux, S.; Schrott, A. G.; Copel, M.; Kellock, A.; Jordan-Sweet, J. *Chem. Mater.* 2006, 18, 6278.
93. Raoux, S.; Welnic, W.; Ielmini, D. *Chem. Rev.* 2010, 110, 240.
94. Krusin-Elbaum, L.; et al. *Appl. Phys. Lett.* 2007, 90, 141902.
95. Ahn, D.; et al. *European Phase-Change and Ovonics Symposium*, 2010, 87.

Dr. M. Anbarasu received his doctoral degree at the department of Instrumentation and Applied physics, Indian Institute of Science, Bangalore, India in 2008. He received the Dr. Srinivasa Rao Krishnamurthy award for the best Ph.D. thesis. He has been working as a post doctoral researcher at the Institute of physics, University of Technology, RWTH, Aachen, Germany since September 2009, sponsored by the Alexander von Humboldt foundation. His research interest focused on the properties and characterization of phase change materials and also understanding threshold switching characteristics in slow & fast crystallizing phase change materials.

Professor Dr. Matthias Wuttig has been a Full Professor of Physics at the RWTH University of Technology, Aachen, Germany since 1997 and a JARA-Professor at Research Center Jülich. He is the speaker of the strategy board of RWTH (since 2009) and was Dean of the Faculty of Science, Mathematics and Computer Sciences (2006–2008). He was the recipient of the Stanford R. Ovshinsky award in 2007 and an Einstein Professorship of the Chinese Academy of Sciences in 2009. He leads the Research Group: Physics of Novel Materials, which characterizes and investigates novel materials with unique optical and electronic properties. Recently this research has focused on the explanation of the unique property portfolio of phase change materials.